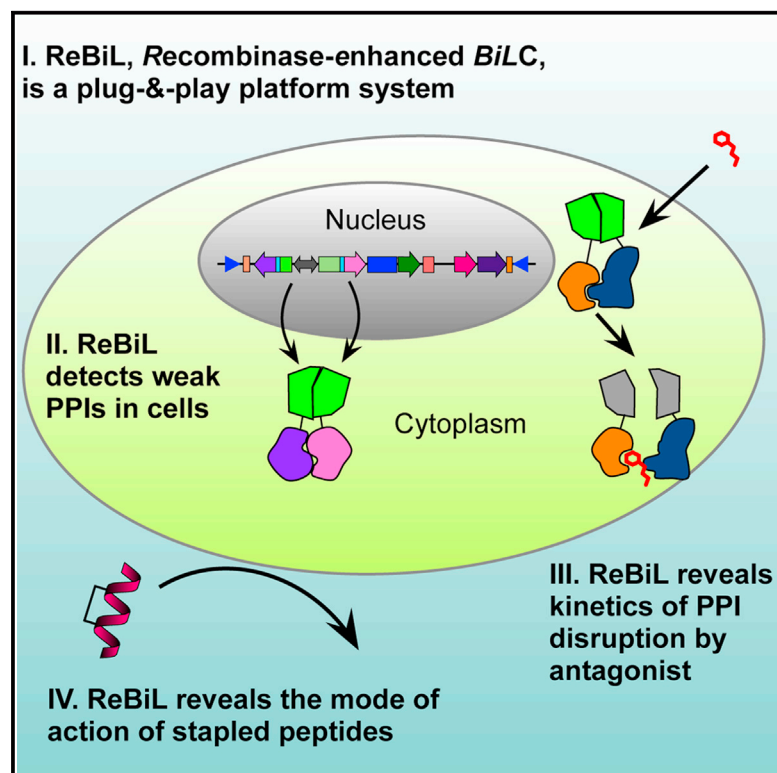# Cell Reports

A Versatile Platform to Analyze Low-Affinity and Transient Protein-Protein Interactions in Living Cells in Real Time

Graphical Abstract

I. ReBiL, *R*ecombinase-enhanced *BiL*C, is a plug-&-play platform system

II. ReBiL detects weak PPIs in cells

Nucleus

Cytoplasm

III. ReBiL reveals kinetics of PPI disruption by antagonist

IV. ReBiL reveals the mode of action of stapled peptides

Authors

Yao-Cheng Li, Luo Wei Rodewald, ..., Kenneth F. Wertman, Geoffrey M. Wahl

Correspondence

wahl@salk.edu

In Brief

Li et al. developed a recombinase-enhanced bimolecular luciferase complementation platform, termed ReBiL, to evaluate low-affinity protein-protein interactions (PPIs) that are not detectable by other methods and to analyze PPI antagonists in living cells. ReBiL showed that small-molecule p53-Mdm2 antagonists disrupt their intended targets effectively in cells, whereas stapled peptides did not. Stapled peptides unexpectedly induced cell membrane disruption resulting in p53-independent death associated with cytoplasmic leakage. ReBiL is also valuable for high-throughput screening and for deciphering signaling mechanisms mediated by protein interactions.

Highlights

ReBiL is able to detect low-affinity, transient protein-protein interactions in cells

ReBiL has a superior signal-to-noise ratio compared to other available methods

ReBiL reveals the kinetics of PPI disruption by antagonists

ReBiL reveals the mode of action of stapled peptides

CrossMark

CellPress

A Versatile Platform to Analyze Low-Affinity and Transient Protein-Protein Interactions in Living Cells in Real Time

Yao-Cheng Li,[1] Luo Wei Rodewald,[1] Christian Hoppmann,[2] Ee Tsin Wong,[1] Sylvain Lebreton,[3] Pavel Safar,[3] Marcel Patek,[3] Lei Wang,[2] Kenneth F. Wertman,[3] and Geoffrey M. Wahl[1],*

[1]Gene Expression Laboratory, The Salk Institute for Biological Studies, 10010 North Torrey Pines Road, La Jolla, CA 92037, USA
[2]Chemical Biology and Proteomics Laboratory, The Salk Institute for Biological Studies, 10010 North Torrey Pines Road, La Jolla, CA 92037, USA
[3]Sanofi Tucson Innovation Center, 2090 East Innovation Park Drive, Oro Valley, AZ 85755, USA
*Correspondence: wahl@salk.edu
 http://dx.doi.org/10.1016/j.celrep.2014.10.058

SUMMARY

Protein-protein interactions (PPIs) play central roles in orchestrating biological processes. While some PPIs are stable, many important ones are transient and hard to detect with conventional approaches. We developed ReBiL, a recombinase enhanced bimolecular luciferase complementation platform, to enable detection of weak PPIs in living cells. ReBiL readily identified challenging transient interactions between an E3 ubiquitin ligase and an E2 ubiquitin-conjugating enzyme. ReBiL's ability to rapidly interrogate PPIs in diverse conditions revealed that some stapled α-helical peptides, a class of PPI antagonists, induce target-independent cytosolic leakage and cytotoxicity that is antagonized by serum. These results explain the requirement for serum-free conditions to detect stapled peptide activity, and define a required parameter to evaluate for peptide antagonist approaches. ReBiL's ability to expedite PPI analysis, assess target specificity and cell permeability, and reveal off-target effects of PPI modifiers should facilitate the development of effective, cell-permeable PPI therapeutics and the elaboration of diverse biological mechanisms.

INTRODUCTION

Most cellular functions are conducted by interactions between multiple proteins comprising either static or dynamic macromolecular machines. Dynamic protein-protein interactions (PPIs) are often composed of weak and transient interactions that render their discovery and analysis in physiologically relevant environments difficult. The human protein "interactome" may involve ~130,000–650,000 PPIs (Stumpf et al., 2008; Venkatesan et al., 2009). Even if only a small fraction of these PPIs cause

disease through aberrant interactions (Ivanov et al., 2013), the availability of rapid PPI antagonist screens would open up vast new opportunities for developing therapeutic agents. Although fluorescent-image-based assays such as the proximity ligation in situ assay (P-LISA) (Söderberg et al., 2006; Bernal et al., 2010) and two- or three-hybrid assays have been used to evaluate PPI antagonists in cells (Brown et al., 2013; Herce et al., 2013), they do not enable simultaneous evaluation of on-target validation and facile, high-throughput analysis of target disruption in living cells. Clearly, methods that would enable real-time detection of PPIs and direct measurement of their intracellular disruption by antagonists are needed. To address this need, we integrated Cre-recombinase *m*ediated *c*assette *e*xchange (RMCE) (Wong et al., 2005) and bimolecular luciferase complementation (BiLC) (Luker et al., 2004) in an inducible gene-expression format to create a platform system for detecting and analyzing PPIs. We refer to this approach as recombinase-enhanced BiLC and use the acronym ReBiL for concision as well as to precisely and simply describe the integration of its key components.

We applied ReBiL to two outstanding problems to assess the potential breadth of biological problems it could be used to study. First, we evaluated its ability to detect weak, transient PPIs in living cells, as exemplified by the interaction of the E2 ubiquitin-conjugating enzyme UBE2T and FANCL, the E3 ubiquitin ligase to which it binds. FANCL is a critical component of the Fanconi anemia DNA repair pathway. Mutations in this pathway cause hematologic abnormalities and create a predisposition to develop cancer (Moldovan and D'Andrea, 2009). E2-E3 interactions are usually transient and typically occur in the low micromolar range (Deshaies and Joazeiro, 2009; Ye and Rape, 2009), which makes their interaction difficult to detect. Although the interaction between UBE2T and FANCL E3 ligase was shown in a yeast two-hybrid screen (Machida et al., 2006), it has eluded detection in living mammalian cells. The UBE2T-FANCL dissociation constant was measured as 0.454 μM by isothermal titration calorimetry, but this required analysis at 8°C (Hodson et al., 2011). Furthermore, it was shown that cocrystallization of UBE2T and FANCL required their fusion (Hodson et al., 2014), consistent

with the fact that they associate with low affinity. Therefore, using ReBiL to assess the association of UBE2T and FANCL provides a stringent test of its ability to detect such challenging interactions.

The second system to which we applied ReBiL involves the p53 tumor suppressor. Defects in the p53 pathway occur in as many as 22 million cancer patients, and ∼50% of these defects are due to inactivating mutations in p53 itself (Brown et al., 2009). Many of the remaining tumors contain alterations that lead to overexpression of either of two oncogenes (Mdm2 and Mdm4) that bind to wild-type p53 and inactivate it by serving as an E3 ubiquitin ligase (Mdm2) and/or a transcriptional repressor (Mdm2 and Mdm4). Therefore, drugs that could interfere with p53-Mdm2 and p53-Mdm4 interactions could restore p53 function and significantly benefit patients whose cancers express wild-type p53 (Brown et al., 2009; Wade et al., 2013).

Unlike classic enzyme-ligand-binding pockets that can be effectively targeted by small molecules, the surfaces on which protein domains interact are typically large, flat, and featureless (Wells and McClendon, 2007). Nevertheless, several PPI antagonists that disrupt p53-Mdm2, p53-Mdm4, or both have been reported (Brown et al., 2009; Wade et al., 2013). Recently, stapled α-helical (SAH) peptides have been designed and suggested as the model for superior PPI antagonists because of their larger interaction interfaces, better structural stability, protease resistance, and cell permeability (Verdine and Hilinski, 2012). Conventionally, the effectiveness of a PPI antagonist has been evaluated by means of in vitro biochemical and biophysical assays that quantify the ability of the antagonist to displace one of the interacting protein fragments. However, such assays do not reveal whether molecules that work effectively in in vitro systems can cross the cell membrane to effect target disruption in a native intracellular environment. While fluorescence-activated cell sorting (FACS) analyses have been used to indicate whether fluorophore-tagged PPI antagonists can enter cells, they do not reveal the subcellular localization (e.g., endosome versus cytoplasm) of the antagonists or whether they reach their targets at concentrations sufficient to disrupt the PPIs and elicit biological effects. Furthermore, assays of biologic activities such as cell death can be misleading and do not provide direct evidence of the intracellular efficacy of a PPI antagonist. For example, since p53 can be activated by diverse cellular insults and many different mechanisms (Beckerman and Prives, 2010), the ability of a putative PPI antagonist to activate p53 target genes or p53-dependent biological processes does not prove that these effects were directly mediated by disruption of p53-Mdm2 and/or p53-Mdm4 complexes.

Here, we report that ReBiL can detect transient and weak PPIs, such as those between UBE2T and FANCL. Additionally, ReBiL enabled us to elucidate on- and off-target activities of SAH peptides, as well as a mechanism by which serum antagonizes SAH-peptide-induced membrane damage. Because of its sensitivity, specificity, and versatility, the ReBiL platform should find broad applications for elucidating biological mechanisms and screening for small-molecule- and peptide-based PPI antagonists.
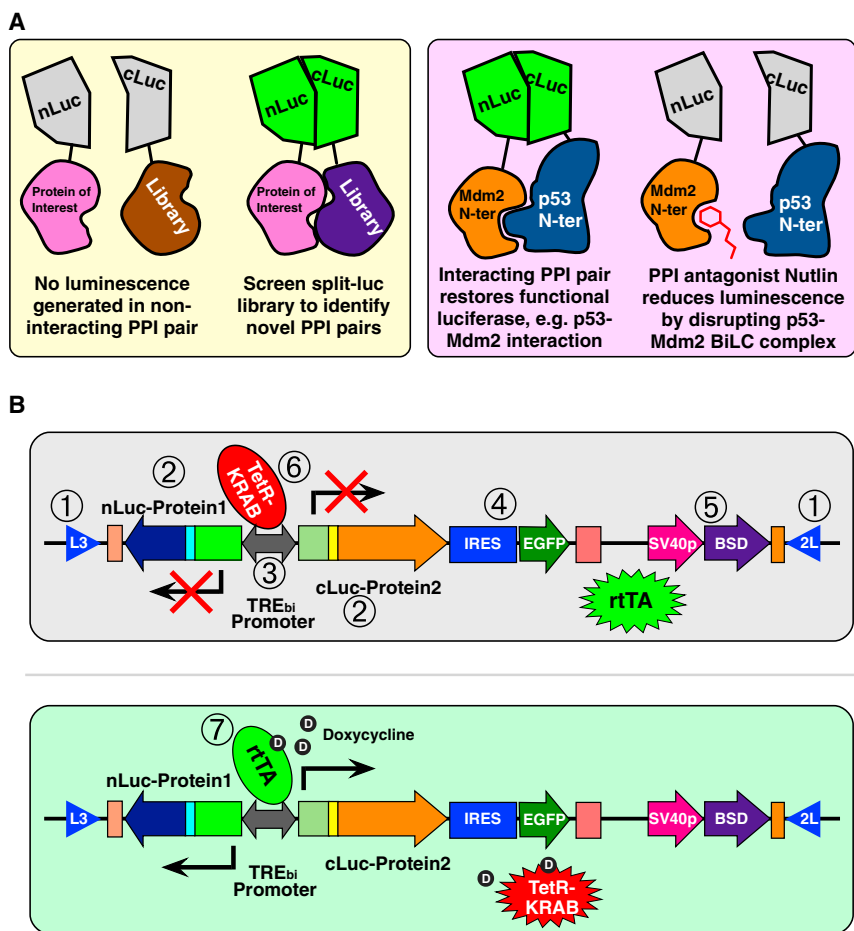
RESULTS

Development of the ReBiL Platform System

We use the firefly BiLC (Luker et al., 2004), a type of protein-fragment complementation assay (PCA) (Michnick et al., 2007), to study PPIs and their antagonists because it has two unique advantages. First, the lack of background luminescence in mammalian cells creates an opportunity for high sensitivity. Second, while split fluorescent proteins associate irreversibly, firefly split luciferase fragments exhibit little if any interaction by themselves, enabling rapid dissociation of complementing pairs (Yang et al., 2009; Ilagan et al., 2011; Macdonald-Obermann et al., 2012). These features make BiLC ideal for analyzing PPI stability and ascertaining the effectiveness of PPI antagonists.

Firefly luciferase PCA relies on the reconstitution of luciferase enzymatic activity from two split fragments and the interaction of the proteins to which they are genetically fused (Luker et al., 2004; Figure 1A). Typical BiLC experiments utilize transient transfection of two plasmids encoding each split luciferase fusion partner (Luker et al., 2004; Paulmurugan and Gambhir, 2007; Cassonnet et al., 2011; Gilad et al., 2014). Consequently, the sensitivity, accuracy, and reproducibility of these experiments are profoundly influenced by the percentage of cells that have been transfected and the copy numbers of each expressed plasmid. Alternatively, one can also perform BiLC after selecting for stable cell clones that carry both split luciferase fusions, such as in studies of EGF receptors and the Notch pathway (Yang et al., 2009; Ilagan et al., 2011; Macdonald-Obermann et al., 2012). However, screening and identifying stable clones with appropriate expression levels is often time-consuming and labor intensive, and does not enable the generation of isogenic lines to compare the activities of mutant and wild-type alleles.

We overcame these drawbacks by generating the ReBiL platform (see Table S1 for feature descriptions). Cre recombinase is used to insert a ReBiL targeting cassette encoding both split luciferase fusion partners into a predetermined floxed acceptor locus integrated at a single chromosomal site in host cells (Wong et al., 2005; Green et al., 2013; Figure S1). High RMCE integration efficiency and faithful transgene expression at a predetermined genomic locus (Wong et al., 2005) circumvent the tedious and costly processes involved in screening reporter clones generated by random integration or viral infection. This greatly accelerates the production of stable reporter cell lines and enables the routine generation of nine to 12 stable ReBiL cell lines in 4–6 weeks with minimum effort, and could likely be scaled up with the use of robotics.

The ReBiL platform provides two other significant experimental and analytical advantages over other stable clones. First, it facilitates structure, function, and interaction analyses because it enables BiLC fusions encoding wild-type and mutant proteins to be integrated into and expressed homogeneously from the same chromosomal locus (Figure S1). Second, single-copy integration and doxycycline-tunable regulation of transgenes (Figure 1B) generate rheostatic and uniform expression (Rossi et al., 2000; Wong et al., 2005) that can be tuned to physiologically relevant levels. Together, these implementations

Figure 1. Description of the ReBiL Platform System and Expected Results Generated by PPIs and Antagonists

(A) Cartoon depicting the BiLC strategy to detect PPIs and their disruption by antagonists.

(B) Expression of a ReBiL cassette was controlled by both TetR-KRAB in the absence of doxycycline (top panel) and rtTA2^S-M2 in the presence of doxycycline (bottom panel). The numbers in open circles indicate each key component in the ReBiL platform system (see Table S1).

See also Figure S1.

We also note that UBE2T and FANCL expression did not affect cell viability (Figure 2D). Thus, the absence of BiLC signal in the UBE2T and FANCL_C307A cells must result from their inability to interact rather than a difference in protein level and cell viability. The very low BiLC signals from the random integrant pool (Figure 2A, right) correlates with the low expression levels of the BiLC pairs (Figure 2B), consistent with a recent report showing that PPIs depend strongly on abundance (Levy et al., 2014). It is especially significant, therefore, that ReBiL manifests a robust signal-to-noise ratio between these weakly interacting proteins even when at least one of them is expressed at lower than endogenous levels.

Intriguingly, at lower temperature (30°C), both ReBiL and random integrated cells generated higher total BiLC signals and signal-to-noise ratios (~10-fold in ReBiL cells; Figure S2B) without much difference in the levels of expressed split luciferase fusions (Figure S2C) compared with 35°C (Figure 2B). Similarly, the expressed split-luciferase-UBE2T fusion was less abundant than endogenous UBE2T endogenous UBE2T at 30°C (Figure S2D), and no growth differences between wild-type and mutant cells were observed (data not shown). This temperature dependency is consistent with the low affinity of these interacting proteins and may indicate that at 30°C, UBE2T-FANCL has a lower dissociation rate (higher affinity). Importantly, at both temperatures, the ReBiL platform exhibited a significantly enhanced ability to detect weak and transient PPIs.

Analysis of Protein Interactions in the p53 Pathway using ReBiL

Several small-molecule- and peptide-based compounds have been reported to interfere with p53-Mdm2 and p53-Mdm4 interactions in biophysical assays and to activate p53 in living cells (Brown et al., 2009; Wade et al., 2013). However, recent data have raised questions about the ability of some SAH peptides to interfere with p53-Mdm2 and p53-Mdm4 interactions in cells (Brown et al., 2013). Therefore, we used the ReBiL system to evaluate small-molecule-, SAH peptide-, and cyclotide-based p53-Mdm2 and p53-Mdm4 PPI antagonists.

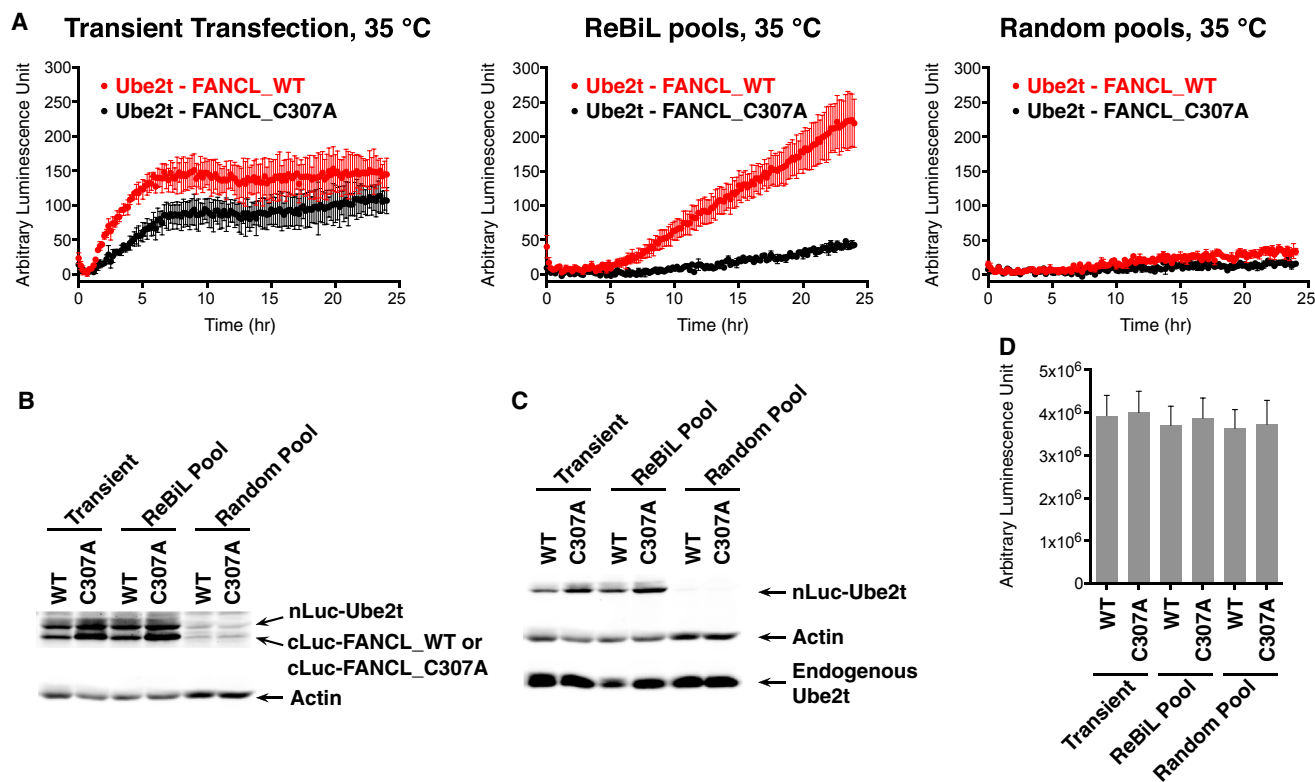significantly enhance the reproducibility and signal-to-noise ratio of the firefly luciferase PCA.

ReBiL Enhances Detection of Weak PPIs

We compared BiLC signals generated by transient transfection, ReBiL, and random integration approaches. We used the identical inducible reporter constructs encoding either UBE2T and FANCL or UBE2T and the FANCL_C307A mutation (Figure S2A; Table S2). FANCL-C307A is a RING domain mutation that prevents interaction with UBE2T (Machida et al., 2006) and serves as a negative control. The luminescent signals generated in transiently transfected cells and random integrants were barely statistically different between the specific interaction pair (UBE2T-FANCL) and the mutant pair (UBE2T-FANCL_C307A) (Figure 2A). In stark contrast, the UBE2T-FANCL ReBiL cells generated ~5-fold higher luminescent signals than the UBE2T-FANCL_C307A mutant ReBiL cells (Figure 2A, middle panel) at 35°C. The expression levels of FANCL_C307A were higher than those of its wild-type counterpart, which corresponded to increased levels of UBE2T, regardless of whether transfection or ReBiL was used (Figure 2B). Importantly, the level of introduced UBE2T was always lower than that of the endogenously produced protein (Figure 2C), but due to a lack of validated FANCL antibody, we could not evaluate its endogenous level.

Figure 2. Detection of Low-Affinity UBE2T and FANCL Interaction with ReBiL

(A) ReBiL detected UBE2T and FANCL interaction with a significantly higher signal-to-noise ratio. Luminescent signals in the transient transfection, ReBiL, and randomly integrated reporter cells were compared at 35°C. Data shown are mean ± SEM from three independent experiments.

(B) Western blot analysis of BiLC fusion proteins. nLuc-HA-UBE2T, cLuc-FLAG-FANCL_WT, and cLuc-FLAG-FANCL_C307A were detected by anti-HA and anti-FLAG, respectively. Actin served as a loading control.

(C) Western blot analysis of the levels of nLuc-UBE2T and endogenous UBE2T by anti-UBE2T (Cell Signaling). Actin served as a loading control.

(D) CellTiter-Glo assay indicated there was no growth difference between FANCL_WT and FNACL_C307A cells. Data shown are mean ± SEM from three independent experiments.

See also Figure S2.

We used two strategies to avert cytotoxicity or cell-cycle arrest that could be generated by wild-type p53 activation. First, we used p53 null Saos-2 cells as the host for the ReBiL reporter cell line. Second, we combined two p53 mutations, the R273H (Joerger and Fersht, 2008) and C312 truncation (Vassilev et al., 2004), to build a transcriptionally inactive split luciferase p53 fusion that could interact with Mdm2 and Mdm4 (Figure S3A; Table S2).

We evaluated the specificity of ReBiL for studying p53-Mdm2 interaction with their antagonist Nutlin-3a, which is known to disrupt p53-Mdm2, but not p53-Mdm4, interactions (Vassilev et al., 2004; Patton et al., 2006; Wade et al., 2008). As expected, Nutlin-3a reduced the p53-Mdm2, but not the p53-Mdm4, BiLC signal (Figure 3A). Signal reduction did not result from Nutlin-3a-induced effects on protein levels (Figure 3B) and cell viability (data not shown). These data demonstrate the specificity of the ReBiL system for discriminating between a small molecule's ability to prevent interaction between p53 and the two very similar binding sites in Mdm2 and Mdm4 in vivo.

Whether small molecules like Nutlin-3a disrupt preformed p53-Mdm2 complexes in living cells has remained an open

question. We used ReBiL to investigate this by first inducing expression of the p53- and Mdm2-split luciferase fusion pairs to generate a functional BiLC complex, and then removing doxycycline to prevent their further transcription. Subsequent incubation of the "preloaded" cells with Nutlin-3a enabled us to analyze the decay of the p53-Mdm2 BiLC complex in living cells. The p53-Mdm2 complexes decayed over time, and this was accelerated significantly and dose dependently by Nutlin-3a (Figure 3C, left panel). Western blotting analysis indicated that Nutlin-3a did not promote degradation of BiLC fusion proteins (Figure 3D, compare lanes 2 and 3). Since doxycycline withdrawal stops p53- and Mdm2-split luciferase fusion transcription, but not translation, we added cycloheximide to prevent translation and then determined dissociation with and without Nutlin-3a. We determined luminescence every minute during a 40 min time period after inhibiting transcription and translation. Similar to what we observed in longer-duration experiments (Figure 3C), Nutlin-3a dose-dependently reduced p53-Mdm2 BiLC signals within 20 min, cycloheximide did not appreciably affect the kinetics (Figure S3B), and p53- and Mdm2-BiLC fusion protein levels remained unchanged during the short time period of the
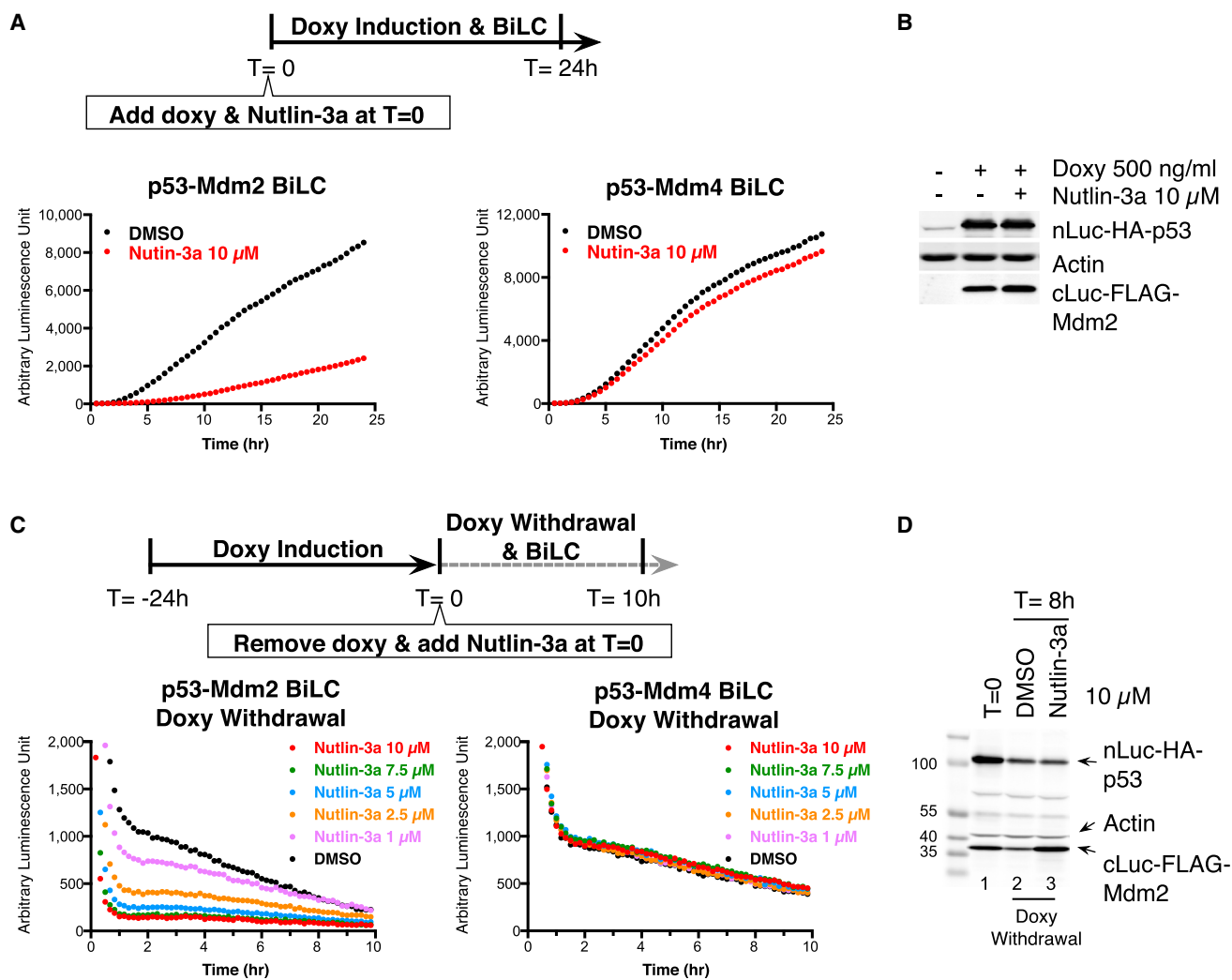
Figure 3. Real-Time BiLC Analyses Faithfully Report PPIs and Activity of the p53-Mdm2 Antagonist

(A) Nutlin-3a prevents newly synthesized p53-Mdm2, but not p53-Mdm4, interactions. Saos-2 p53-Mdm2 and p53-Mdm4 ReBiL cells in 384-well plates (8,500 cells per well) were treated with 500 ng/ml doxycycline, 100 μM D-luciferin, and 10 μM Nutlin-3a or DMSO at time = 0. Luminescence was read every 30 min for 24 hr at 37°C. Data shown are from a representative experiment out of more than three independent experiments.

(B) Western blot analysis of BiLC fusion proteins showed that Nutlin-3a does not affect the expression amounts of nLuc-HA-p53 and cLuc-FLAG-Mdm2 (detected by anti-HA and anti-FLAG, respectively). Actin served as a loading control.

(C) Preinduced Saos-2 p53-Mdm2 and p53-Mdm4 ReBiL cells were reseeded into a 384-well plate (5,000 cells per well) together with Nutlin-3a and D-luciferin at time = 0. The p53-Mdm2 and p53-Mdm4 BiLC signals decayed over time in a biphasic fashion. The first steep decline in BiLC signal is likely due to the temperature changes of the ReBiL cells when moving from the bench (~24°C) to the prewarmed luminometer at 37°C. The second slow-decay phase of BiLC results from doxycycline withdrawal and the consequent reduction in transcription of the BiLC fusion genes. Luminescence was read every 10 min for 10 hr at 37°C. Data shown are from a representative experiment out of more than three independent experiments.

(D) Western blot analysis showed that Nutlin-3a did not promote nLuc-HA-p53 and cLuc-FLAG-Mdm2 degradation. Actin was a loading control.

See also Figure S3.

analysis (Figure S3C). The p53-Mdm4 complexes were not affected by Nutlin-3a regardless of cycloheximide addition (Figure S3D). These data show that small-molecule PPI antagonists such as Nutlin-3a can selectively and rapidly disrupt preformed p53-Mdm2 complexes in living cells.

Disruption of p53-Mdm4 complexes has been an important goal for reactivation of wild-type p53 in cancer therapy (Wade et al., 2013). We used ReBiL to determine whether a previously reported small-molecule p53-Mdm4 antagonist, SJ-172550

(Reed et al., 2010), disrupts this interaction in cells. No decrease in p53-Mdm4 BiLC signal was detected (Figure S3E). We then evaluated a second compound, RO-5963, that has been proposed to disrupt both p53-Mdm2 and p53-Mdm4 interactions by increasing Mdm2-Mdm4 association (Graves et al., 2012). Consistent with this model, RO-5963 increased the BiLC signal in the Mdm2-Mdm4 N-terminal BiLC pair (Figures S3F and S3G). However, even though the Mdm2 binding affinity of RO-5963 (17.3 nM) is similar to that of Nutlin-3a (18.7 nM)
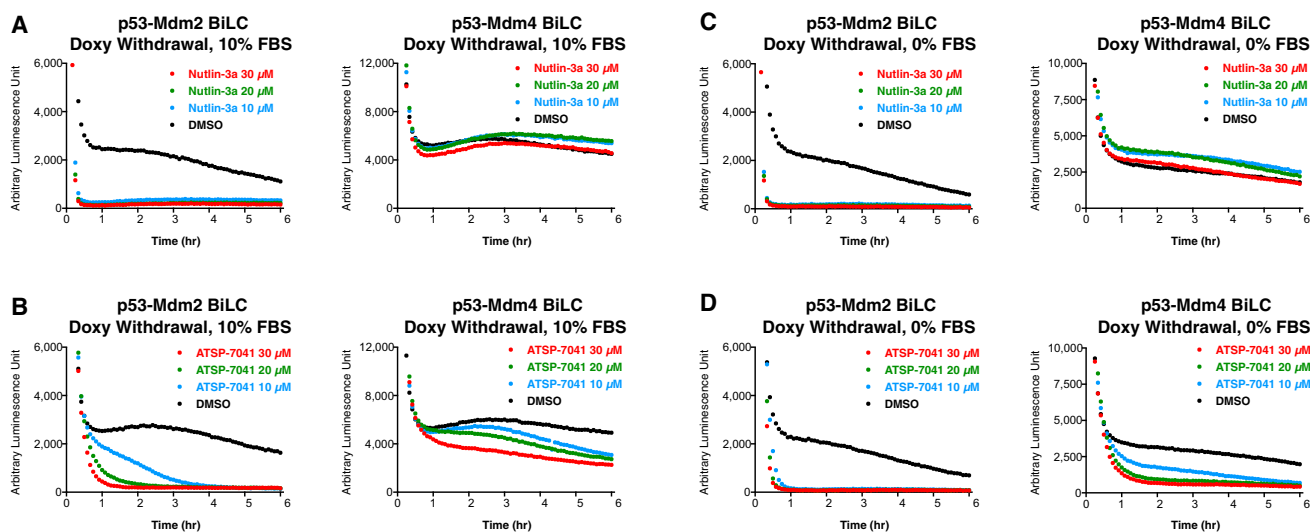
Figure 4. Analysis of the Ability of SAH Peptides to Disrupt p53-Mdm2 and p53-Mdm4 Complexes in Living Cells, and Antagonism by Serum
(A–D) Saos-2 p53-Mdm2 and p53-Mdm4 ReBiL cells in 96-well plates (20,000 cells per well) were preinduced by doxycycline (500 ng/ml for 24 hr). At time = 0, cells were washed with DMEM and treated with new media containing different PPI antagonists with or without 10% FBS. Luminescent signals were read every 5 min for 6 hr in a Tecan-M200 microplate reader at 37°C. The ReBiL cells were treated with (A) Nutlin-3a and 10% FBS, (B) ATSP-7041 and 10% FBS, (C) Nutlin-3a and no FBS, and (D) ATSP-7041 and no FBS. Data shown are from a representative experiment out of more than three independent experiments. See also Figure S4.

(Graves et al., 2012), RO-5963 exhibited a limited ability to disrupt the p53-Mdm2 complex and no effect on the p53-Mdm4 complex in living cells (Figure S3H). Intriguingly, although Nutlin-3a binds to the same Mdm2 N-terminal domain as RO-5963 (Graves et al., 2012), it did not promote Mdm2 and Mdm4 N-terminal domain interactions (Figure S3G, right panel). These data demonstrate the exquisite specificity of the ReBiL strategy for revealing both the agonist and antagonist activities of putative PPI modifiers in vivo.

SAH Peptides Do Not Efficiently Disrupt p53-Mdm2 and p53-Mdm4 Interactions in Living Cells
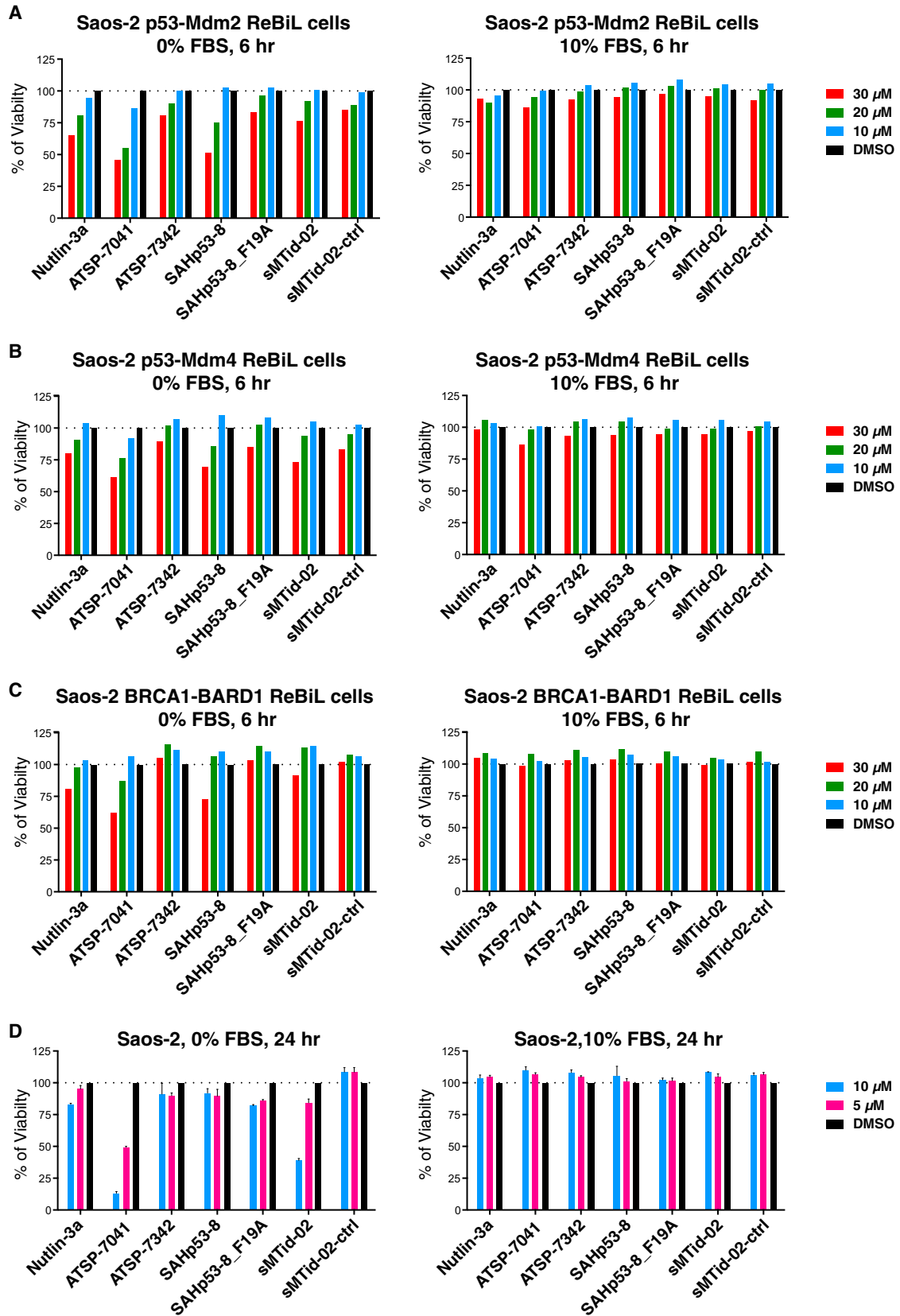
We next determined whether the ability of SAH peptide-based antagonists that have been shown to disrupt p53-Mdm2 and p53-Mdm4 interactions in vitro also do so in living cells. We analyzed SAHp53-8 (Bernal et al., 2007, 2010), sMTide-02 (Brown et al., 2013), and ATSP-7041 (Chang et al., 2013). The larger binding surfaces of these peptidic drugs confer far higher binding affinities than Nutlin-3a, as exemplified by ATSP-7041 with a Ki = 0.9 nM for Mdm2 compared with Ki = 52 nM for Nutlin-3a (determined by Chang et al., 2013). Surprisingly, despite this much higher binding affinity, SAH peptides are typically used at higher concentrations (20–100 μM) to elicit cellular activities (Bernal et al., 2010; Gembarska et al., 2012; Chang et al., 2013; Brown et al., 2013). Indeed, in spite of its 57-fold higher binding affinity, ATSP-7041 (10 μM) reached full p53-Mdm2 inhibition much more slowly (4 hr) than Nutlin-3a (20 min; compare Figures 4A and 4B). ATSP-7041 exhibited only marginal activity against p53-Mdm4 complexes (Figure 4B, right). Surprisingly, SAHp53-8 and sMTide-02 exhibited no detectable ability to disrupt p53-Mdm2 or p53-Mdm4 complexes in living cells (Figures S4B and S4C). Paradoxically, sMTide-02 actually increased BiLC signals in a dose-dependent fashion for both p53-Mdm2 and p53-Mdm4 complexes by an unclear mechanism (Figure S4C).

These results indicate that higher binding affinity in vitro does not necessarily correlate with higher intracellular PPI disruption activity, suggesting that there might be a barrier to effective entry of the SAH peptides into the cells. The increased activity of ATSP-7041 in 0% serum (Chang et al., 2013; Figure 4D) indicates that the serum itself might limit the intracellular access of the SAH peptides, which would be consistent with prior studies in which the cellular activity of SAH peptides was typically measured in serum-free medium (Bernal et al., 2010; Edwards et al., 2013; see Figure S5). Since the mechanism for serum-mediated inhibition of SAH peptides has remained elusive, we investigated this more fully, as described below.
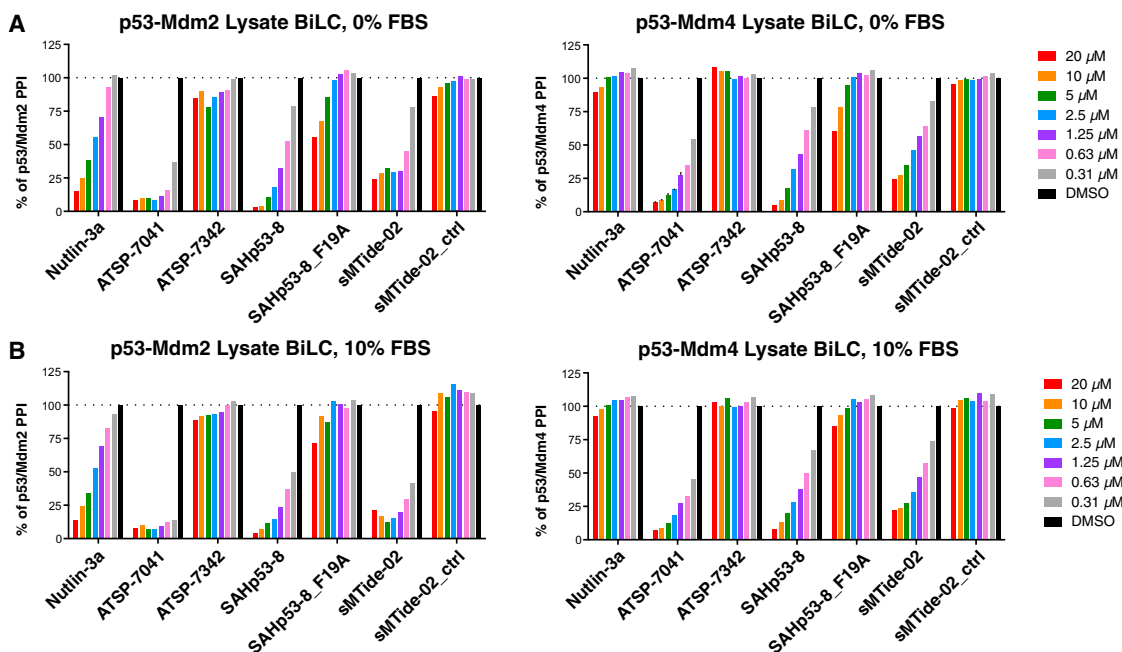
Dual Mdm2 and Mdm4 Antagonist SAH Peptides Exhibit p53-Independent Cytotoxicity

Because the ReBiL system enables real-time analysis of the kinetics of target disruption in cells, we were able to determine when target disruption occurred and then correlate that with other parameters, such as cell viability. We noticed that wild-type SAH peptides rapidly (~6 hr) and dose dependently reduced the viability of p53 null Saos-2 ReBiL cells (Figure 5). This cytotoxicity is p53 independent, since the Saos-2 ReBiL cells are p53 null and they were engineered to encode a transcriptionally inactive split-luciferase p53 fusion protein. This also occurred in Saos-2 cells expressing BRCA1-BARD1 BiLC fusion proteins (Brzovic et al., 2001; Figure 5C; Table S2). Surprisingly, the negative control mutant peptides exhibited neither PPI disruption (Figure S4) nor significantly reduced cell viability, even in serum-free media (Figure 5). Importantly, 10% serum

A Saos-2 p53-Mdm2 ReBiL cells
0% FBS, 6 hr

Saos-2 p53-Mdm2 ReBiL cells
10% FBS, 6 hr

B Saos-2 p53-Mdm4 ReBiL cells
0% FBS, 6 hr

Saos-2 p53-Mdm4 ReBiL cells
10% FBS, 6 hr

C Saos-2 BRCA1-BARD1 ReBiL cells
0% FBS, 6 hr

Saos-2 BRCA1-BARD1 ReBiL cells
10% FBS, 6 hr

D Saos-2, 0% FBS, 24 hr

Saos-2, 10% FBS, 24 hr

(legend on next page)

Figure 6. The BiLC Lysate Assay Reveals that Serum Does Not Prevent SAH Peptides from Disrupting p53-Mdm2 or p53-Mdm4 Complexes

(A) Cellular lysates obtained from p53-Mdm2 and p53-Mdm4 ReBiL cells were coincubated with the indicated PPI antagonists in the absence of FBS in 384-well plates at room temperature for 10 min. Steady-Glo was added, and luminescence was detected at 26°C.

(B) BiLC lysate assays were performed as in (A) except for the inclusion of 10% FBS. The data shown are from a representative experiment out of more than three independent experiments and were normalized to the luminescent reading of DMSO (set to 100%).

See also Figures S6 and S7.

prevented loss of cell viability induced by wild-type SAH peptides (Figure 5) and also reduced the effectiveness of ATSP-7041 (Chang et al., 2013; compare Figures 4B and 4D). Similarly, lower concentrations of ATSP-7041 and sMTide-02 peptides also reduced Saos-2 viability in 24 hr in a serum-dependent manner (Figure 5D). These data imply that these p53-activating SAH peptides can elicit p53-independent cytotoxicity, which is inhibited by serum. As reported previously (Liu et al., 2010), high Nutlin-3a concentrations also induce p53-independent cytotoxicity (Figure 5), likely by off-target effects different from those of SAH peptides (discussed in Figure 7).

Dual Mdm2 and Mdm4 Antagonist SAH Peptides Exhibit Strong Target Disruption Activity in Cell Lysates

We consider the following as two reasonable explanations for serum's ability to both prevent SAH peptide-induced cytotoxicity and reduce the efficacy of PPI disruption: first, serum may bind SAH peptides in such a way as to prevent them from disrupting

their target complexes; second, serum may prevent SAH peptide entry into cells to both reduce their efficacy and limit cytotoxicity.

We gained insights into these possibilities by developing a cell-free BiLC assay. We reasoned that if SAH peptides efficiently disrupt PPIs in cell lysates, but not in intact cells, then membrane penetration and access to their intracellular targets might be limiting. We induced expression of the BiLC complexes by doxycycline and then prepared cell lysates using an optimized buffer (PPI lysis buffer [PLB]; Figure S6). In contrast to in vitro binding competition assays that use purified protein fragments to identify PPI antagonists, the BiLC lysate assay contains all soluble cellular proteins extracted by PLB and therefore should reveal PPI inhibitor potency in a more physiologically relevant context.

Consistent with the cell-based BiLC assay, Nutlin-3a efficiently disrupted p53-Mdm2, but not p53-Mdm4, complexes in the lysate BiLC assay (Figures 6 and S6E). SJ-172550 (Reed et al., 2010), RO-5963 (Graves et al., 2012), and pyrrolopyrimidine

---

Figure 5. Viability Assay of Saos-2 ReBiL Cells Reveals that p53-Activating SAH Peptides Possess p53-Independent Cytotoxicity in the Absence of Serum

(A–C) Cell viability was measured by CellTiter Glo assay at 6 hr after Saos-2 ReBiL cells (A, p53-Mdm2; B, p53-Mdm4; and C, BRCA1-BARD1) were treated with the indicated SAH peptides without and with 10% FBS. The data shown are from a representative experiment out of more than three independent experiments and were normalized to the luminescent reading of DMSO (set to 100%).

(D) Saos-2 cells were treated with the indicated SAH peptides in 384-well plate (2,000 cells per well) without and with 10% FBS for 24 hr. Cell viability was detected by CellTiter Glo assay. The data shown are the mean ± SD from two independent experiments and were normalized to the luminescent reading of DMSO (100%).

See also Figures S5 and S7.
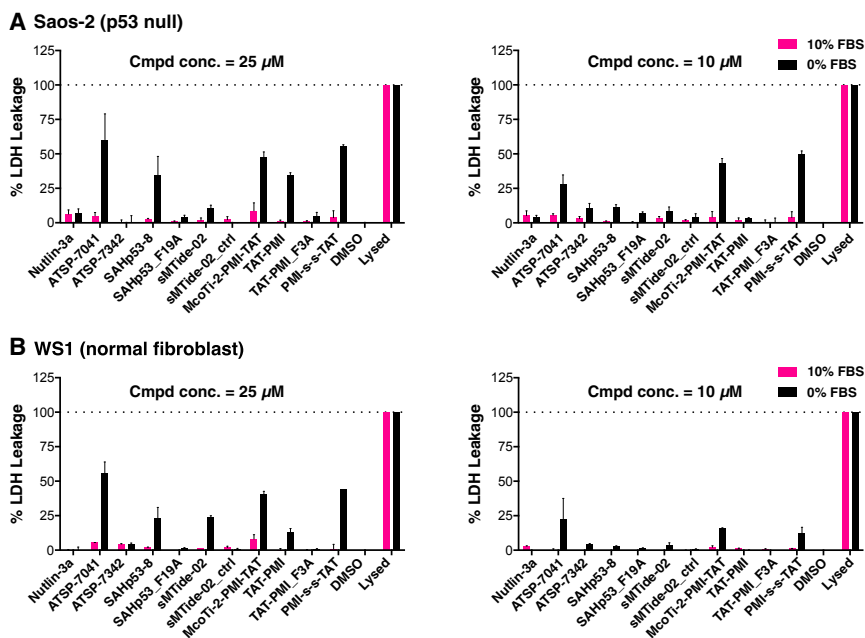
Figure 7. Stapled Peptides Induce Membrane Leakage by a p53-Independent Mechanism that Is Antagonized by Serum

(A) Saos-2 cells were treated with the indicated PPI antagonists at 25 μM and 10 μM for 6 hr. Accumulation of cytoplasmic LDH in the growth medium was used as a metric of cell membrane damage. LDH was detected by the CytoTox 96 Non-Radioactive Cytotoxicity Assay Kit (Promega). The lysed sample represents the maximum LDH leakage in this experiment and its reading was set to 100%. DMSO treatment served as the vehicle control and its value was set to 0%.

(B) Normal human fibroblasts (WS1 cells) were treated exactly as in (A). Data are shown as mean ± SEM from two independent experiments.

See also Table S3.

compound 3b (Lee et al., 2011) exhibited no activity in the lysate BiLC assays (Figure S6E), confirming their poor intracellular PPI disruption activity (Figures S3E and S3H). In contrast, SAHp53-8, sMTide-02, and ATSP-7041 were potent p53-Mdm2 and p53-Mdm4 interaction disruptors in the lysate BiLC assays (Figure 6A), and negative control peptides with mutations in amino acids (Phe, Trp, and Leu) that are known to mediate p53 interactions with Mdm2 and Mdm4 were inactive (Figure 6A). The lack of effect of any of these compounds on BRCA1-BARD1 BiLC excludes the explanation that active SAH peptides are simply luciferase inhibitors (Figure S7). These results demonstrate that SAHp53-8 and sMTide-02 are indeed potent PPI antagonists when they can access their targets. This combination of ReBiL assays in cellular lysates and live cells provides a simple and efficient strategy for quickly assessing the specificity and potency of putative PPI antagonists and indicates when poor activity may derive from inefficient intracellular target access.

The inhibitory effect of serum on SAH peptides could result from direct binding of serum proteins to the peptide (Bird et al., 2014). We added 10% fetal bovine serum (FBS) to the lysate BiLC assays to determine directly whether serum reduces the ability of stapled peptides to disrupt p53-Mdm2 and p53-Mdm4 interactions. Serum did not reduce the potency of ATSP-7041, SAHp53-8, or sMTide-02 in cell lysates (Figure 6B). These results demonstrate that serum components or proteins do not sequester or modify SAH peptides and affect their ability to disrupt the target complexes.

Dual Mdm2 and Mdm4 Antagonist SAH Peptides Cause p53-Independent Cell Membrane Damage

Given the data presented above, we conjectured that serum might compromise the ability of SAH peptides to enter the cell. We also wondered whether there might be a mechanistic linkage between the reduced cytotoxicity and reduced PPI disruption by

SAH peptides in cells exposed to serum-containing medium. We reasoned that if SAH peptides compromise membrane integrity, they should be able to gain access to the cytoplasm and their targets, and, by extension, the serum effect could be explained if it antagonized such membrane effects. We tested this possibility by examining the integrity of membranes after they were exposed to SAH peptides in the presence or absence of 10% serum. We quantified release of the cytosolic enzyme lactate dehydrogenase (LDH) into the culture medium as an indicator of the loss of cell membrane integrity. The data clearly show that ATSP-7041, sMTide-02, and SAHp53-8 all caused LDH leakage in the absence of serum (Figure 7). In contrast, 10% serum protected the cell membrane from the damage induced by these SAH peptides (Figure 7). This cell-membrane-damaging activity is p53 independent, since the LDH assay was performed in p53 null Saos-2 cells (Figure 7A). The membranes of normal human WS1 fibroblasts were also damaged by SAH peptides, indicating that this process is not restricted to cancer cells (Figure 7B). Surprisingly, all three mutant stapled peptides lacked this cell-membrane-damaging activity (Figure 7). Importantly, Nutlin-3a did not induce membrane leakage, excluding the possibility that the cytotoxicity observed when it is used at high concentrations results from membrane damage (Figure 5).

We also examined the activities of several PMI-based p53-Mdm2 and p53-Mdm4 antagonists, as these are high-affinity Mdm2-binding peptides obtained through screening phage display libraries (Pazgier et al., 2009; Table S3; Supplemental Experimental Procedures). The lysate BiLC assay showed that all were highly potent p53-Mdm2 and p53-Mdm4 antagonists (Figure S6F). Unfortunately, they all lacked intracellular p53-Mdm2 and p53-Mdm4 disruption activity in 10% serum media (data not shown). In the absence of serum, all but one (McoTi-1-PMI; data not shown) damaged cell membranes in a p53-independent fashion that was exacerbated by inclusion of TAT-penetrating peptides (Wadia et al., 2004; Figure 7). Taken together, our studies show that serum does not prevent SAH peptides from binding to their targets. Instead, serum protects

cell membranes from being damaged by a previously unrecognized membrane-disrupting activity of wild-type SAH peptides.

DISCUSSION

The ReBiL vectors and cell lines described here constitute a platform system that is able to detect weak and transient PPIs, and elucidate the structure-activity relationships of PPI antagonists and agonists. It is sensitive, specific, and can be used to analyze PPIs in both living cells and cell-free systems. For example, we quickly confirmed that small-molecule Nutlin-3a interferes with p53-Mdm2, but not p53-Mdm4, interactions. In contrast, other published antagonists (SJ-172550 and RO-5963) showed little if any PPI disruption activity in cells. Our observations suggest that the reported p53-activating effects of these compounds may result from induction of other cellular stresses (Beckerman and Prives, 2010), and not completely from p53-Mdm2 or p53-Mdm4 disruption. Therefore, there can be a lack of concordance between in vitro biophysical and biochemical assays and in vivo biological readouts. This highlights the critical importance of using an assay that directly analyzes target disruption in cells to deduce the mechanism of action, such as ReBiL.

The ReBiL approach also led to insights concerning the conflicting results of studies using SAH peptides (Brown et al., 2013; Okamoto et al., 2013, 2014). Considerable effort and resources have been expended to develop SAH peptides as PPI antagonists. Given the difficulty of developing small-molecule p53-Mdm4 disruptors, SAH peptides were developed as dual p53-Mdm2 and p53-Mdm4 antagonists, since Mdm2 and Mdm4 contain similar N-terminal hydrophobic clefts that interact with p53. Consistent with expectations, SAH peptides that target this region were shown to have high binding affinities (Bernal et al., 2010; Chang et al., 2013; Brown et al., 2013) and the ability to disrupt both p53-Mdm2 and p53-Mdm4 complexes in vitro (Figure 6). However, there has been much debate about their cell permeability (Okamoto et al., 2013; Brown et al., 2013) and their ability to elicit p53-dependent biological responses (Brown et al., 2013). For example, in contrast to a previous report (Bernal et al., 2010), a recent study found that the SAHp53-8 lacked cytotoxicity and failed to activate a p53 reporter in cell-based analyses (Brown et al., 2013). Our results clearly show that the stapled peptides SAHp53-8 and sMTid-02 exhibited little to no intracellular activity in the presence or absence of serum (Figures S4B, S4C, S4F, and S4G). This likely accounts for the discordance between their nanomolar binding affinities in vitro and their marginal ability to generate p53-dependent cytotoxic responses. ATSP-7041 did antagonize p53-Mdm2 association, but surprisingly had little effect on p53-Mdm4 complexes. However, high concentrations and long time periods were required for any effects to occur. We suggest that this relates to the ability of ATSP to disrupt membranes, which is partly mitigated by serum, and that its strong affinity for Mdm2 enables it to accumulate to a sufficient intracellular concentration for target disruption, though less efficiently and more slowly than Nutlin-3a.

It has been observed that serum decreases the biological activity of SAH peptides (Edwards et al., 2013; Chang et al., 2013; Brown et al., 2013). Our in vitro analyses demonstrated that serum does not prevent SAH peptides from disrupting either p53-Mdm2 or p53-Mdm4 complexes. The live-cell analyses showed that all wild-type SAH peptides tested possessed the unexpected ability to elicit p53-independent membrane damage that correlated with cytotoxicity. Addition of serum prevented both membrane damage and cytotoxicity. Surprisingly, mutations that replaced an essential phenylalanine with alanine in the α-helical region of each peptide abrogated membrane permeabilization and cytotoxicity. We infer that this derives from the ability of these mutations to alter the hydrophobicity and α-helicity of the peptides (Bernal et al., 2007). Previously, the cytotoxicity of the wild-type SAH peptides was interpreted to derive from p53-dependent activity, since mutant control peptides did not exert this effect (Bernal et al., 2010; Chang et al., 2013; Brown et al., 2013). However, our data show that the lack of effect in these mutant peptides is actually due to their inability to permeabilize membranes. Our data are consistent with a recent microscopic study showing that a fluorescent FAM conjugated mutant (F19A) ATSP peptide exhibited limited cellular permeability compared with the apparent cellular distribution of the wild-type ATSP peptide (see Figure 3 in Chang et al., 2013). This agrees with our conclusion that wild-type SAH peptides access the cytoplasm after first compromising membrane integrity. Taken together, these data show that the observed cytotoxicity of the wild-type SAH peptide does not completely depend on functional p53, and the absence of activity in the mutant peptide is related more to its biophysical properties than to its inability to interact with Mdm2 and Mdm4.

We speculate that membrane disturbance may commonly result from positively charged cell-penetrating peptides (CPPs) appended to peptides with exposed hydrophobic residues. For example, the stapled PMI-PenArg (a lysine-to-arginine derivative of the CPP penetratin) elicited cell death within 3 hr in cells growing in serum-free media (data not shown). Similarly, the cationic cell-penetrating D-peptide ^{D}PMI-γ-^{D}R9 rapidly induced p53-independent cytotoxicity (Liu et al., 2010). The positively charged CPPs from N-terminal prion proteins also elicited membrane leakage in defined large unilamellar phospholipid vesicles (Magzoub et al., 2005). It is also worth noting that the unstapled ^{D}PMI-γ-^{D}R9 (Liu et al., 2010), TAT-PMI, and PMI-s-s-TAT peptides induce severe membrane damage (Figure 7) and cytotoxicity, indicating that chemical stapling per se is not required for cytotoxicity (Okamoto et al., 2014).

The ReBiL strategy provides a facile platform system for PPI analyses. We have shown that this system can detect interactions between UBE2T-FANCL (Figure 2), p53-Mdm2, p53-Mdm4 (Figure 3), Mdm2-Mdm4 RING domains (Figure S6), and BRCA1-BARD1 RING domains (Figures 5C and S7), among other proteins (Y.-C.L. and G.M.W., unpublished data). Furthermore, the very high signal-to-noise ratio in the lysate format enabled ReBiL to be used for high-throughput drug screens in a 1,536-well format with Z′ values exceeding 0.7 (Y.-C.L., G.M.W., and K.F.W., unpublished data). We expect ReBiL to have broad applications ranging from identifying noncoding RNAs that facilitate cytosolic PPIs to assessing factors that impact plasma membrane-associated KRAS dimerization, neither of which is feasible using other strategies, such as the two-/three-hybrid systems with transcriptional readouts. Together, these attributes should enable ReBiL to broaden our

understanding of the impact of disease-relevant mutations on protein interactions, elucidate the mechanisms of drug action more precisely, improve the efficacy of PPI antagonists, and advance our understanding of the makeup of the human protein interactome.

EXPERIMENTAL PROCEDURES

Construction of ReBiL Targeting Plasmids
We used standard molecular biology methods and the Gibson Assembly strategy (E2611S; New England Biolabs) to construct all of the ReBiL targeting plasmids. See Table S2 for details.

Real-Time BiLC Assay in Living Cells
Phenol-red free Dulbecco's modified Eagle's medium (DMEM)/F12 (Life Technologies or Sigma-Aldrich) containing 2× concentrated reagents, including doxycycline (Sigma-Aldrich) and D-luciferin (potassium salt, L-8220; Biosynth), were pipetted into a 384-well plate (Corning) at 20 μl per well. The cells were trypsinized and cell numbers were determined. The required number of cells were collected into 1.5 ml LoBind tubes (Eppendorf) and spun at 200 rcf for 5 min at room temperature. The cells were resuspended with DMEM/F12 (phenol-red free) and 20 μl of cells were pipetted into each well. The final concentration of each component was as follows: FBS 10%, ciprofloxacin 10 μg/ml, doxycycline 0–500 ng/ml, and D-luciferin 100–200 μM (5,000–20,000 cells per well). The plate was sealed with MicroAmp Optical Adhesive Film (Life Technologies) and luminescence was read in a Tecan M200 microplate reader (integration time 2 s, 10–30 min per cycle for a total of 24–48 hr at the indicated temperature).

Doxycycline Withdrawal Strategy to Enable Real-Time BiLC Analysis of Protein Complex Dissociation
To evaluate small-molecule PPI antagonists, the ReBiL cells were first cultured in 10- to 15-cm dishes with regular media containing doxycycline (500 ng/ml) and D-luciferin (100 μM) for 24 hr. The next day, the cells were trypsinized and cell numbers were determined. Cells were seeded into assay plates as described above except that doxycycline was eliminated from the media. To evaluate SAH peptides, the cells were seeded into a 96-well plate (Corning) at 20,000 cells per well and incubated in the presence of doxycycline (500 ng/ml) and D-luciferin (100 μM) for 24 hr. The next day, the media were aspirated, cells were washed once with DMEM, and 50 μl of DMEM/F12 (phenol-red free) media containing D-luciferin (100 μM) and the stapled peptides at the indicated concentrations was added into each well. The plate was sealed with MicroAmp Optical Adhesive Film and luminescence was read in a Tecan M200 microplate reader (integration time 2 s, 5–10 min per cycle for a total of 6 hr at 37°C).

Cell Viability Assay
Luminescence-based cell viability assays were performed using CellTiter Glo (Promega), which measures the amount of ATP produced by viable cells, according to the manufacturer's protocol. Luminescence was detected in a Tecan M200 microplate reader with an integration time of 0.5 s. Trypsinized cells were treated with Trypsin inhibitor (Sigma-Aldrich) and then seeded into serum-free media for viability assays.

BiLC Assay using Cell Lysates
Saos-2 or U2OS ReBiL cells were cultured in regular media with doxycycline (500 ng/ml, 48–72 hr). The 4× concentrated drugs diluted in DMEM/F12 media were pipetted into 384-well plates at 10 μl per well. Cells with loaded BiLC complexes were washed and lysed with PLB buffer (100 mM Tris-HCl [pH 7.5], 0.5 mM EDTA, 150 mM NaCl, 0.1% Triton X-100, 1 mM sodium orthovanadate, 50 mM sodium fluoride, and Roche Complete Mini Protease Inhibitor Cocktail). The cell lysates were transferred into 1.5 ml tubes and cleared by centrifugation (13,000 rcf, 5 min at 4°C). The clear lysates were collected and diluted with DMEM (~300 μl DMEM added into 100 μl lysates). Then 10 μl of diluted lysates was immediately pipetted into each of the 384-well plates containing drugs, and the plates were incubated at room temperature for 10 min. Finally, 20 μl

of luciferin reagents (Bright-Glo E2620 or Steady-Glo E2520, Promega) was added into each well and luminescence was read in a Tecan M200 microplate reader (integration time 0.5 s, 3–5 min per cycle for 30 min at 26°C).

LDH Leakage Assay
LDH leakage was detected with the CytoTox 96 Non-Radioactive Cytotoxicity Assay Kit (Promega) per the manufacturer's protocol. For details, see the Supplemental Experimental Procedures.

SUPPLEMENTAL INFORMATION

Supplemental Information includes Supplemental Experimental Procedures, seven figures, and three tables and can be found with this article online at http://dx.doi.org/10.1016/j.celrep.2014.10.058.

AUTHOR CONTRIBUTIONS

Y.-C.L. and G.M.W. conceived the study and designed experiments. Y.-C.L. and L.W.R performed experiments. C.H., E.T.W., S.L., P.S., M.P., L.W., and K.F.W. contributed reagents. Y.-C.L. and G.M.W. analyzed data and wrote the paper with input from all of the authors.

ACKNOWLEDGMENTS

REFERENCES

Beckerman, R., and Prives, C. (2010). Transcriptional regulation by p53. Cold Spring Harb. Perspect. Biol. 2, a000935.

Bernal, F., Tyler, A.F., Korsmeyer, S.J., Walensky, L.D., and Verdine, G.L. (2007). Reactivation of the p53 tumor suppressor pathway by a stapled p53 peptide. J. Am. Chem. Soc. 129, 2456–2457.

Bernal, F., Wade, M., Godes, M., Davis, T.N., Whitehead, D.G., Kung, A.L., Wahl, G.M., and Walensky, L.D. (2010). A stapled p53 helix overcomes HDMX-mediated suppression of p53. Cancer Cell 18, 411–422.

Bird, G.H., Gavathiotis, E., LaBelle, J.L., Katz, S.G., and Walensky, L.D. (2014). Distinct BimBH3 (BimSAHB) stapled peptides for structural and cellular studies. ACS Chem. Biol. 9, 831–837.

Brown, C.J., Lain, S., Verma, C.S., Fersht, A.R., and Lane, D.P. (2009). Awakening guardian angels: drugging the p53 pathway. Nat. Rev. Cancer 9, 862–873.

Brown, C.J., Quah, S.T., Jong, J., Goh, A.M., Chiam, P.C., Khoo, K.H., Choong, M.L., Lee, M.A., Yurlova, L., Zolghadr, K., et al. (2013). Stapled peptides with improved potency and specificity that activate p53. ACS Chem. Biol. 8, 506–512.

Brzovic, P.S., Rajagopal, P., Hoyt, D.W., King, M.C., and Klevit, R.E. (2001). Structure of a BRCA1-BARD1 heterodimeric RING-RING complex. Nat. Struct. Biol. *8*, 833–837.

Cassonnet, P., Rolloy, C., Neveu, G., Vidalain, P.O., Chantier, T., Pellet, J., Jones, L., Muller, M., Demeret, C., Gaud, G., et al. (2011). Benchmarking a luciferase complementation assay for detecting protein complexes. Nat. Methods *8*, 990–992.

Chang, Y.S., Graves, B., Guerlavais, V., Tovar, C., Packman, K., To, K.H., Olson, K.A., Kesavan, K., Gangurde, P., Mukherjee, A., et al. (2013). Stapled α-helical peptide drug development: a potent dual inhibitor of MDM2 and MDMX for p53-dependent cancer therapy. Proc. Natl. Acad. Sci. USA *110*, E3445–E3454.

Deshaies, R.J., and Joazeiro, C.A. (2009). RING domain E3 ubiquitin ligases. Annu. Rev. Biochem. *78*, 399–434.

Edwards, A.L., Gavathiotis, E., LaBelle, J.L., Braun, C.R., Opoku-Nsiah, K.A., Bird, G.H., and Walensky, L.D. (2013). Multimodal interaction with BCL-2 family proteins underlies the proapoptotic activity of PUMA BH3. Chem. Biol. *20*, 888–902.

Gembarska, A., Luciani, F., Fedele, C., Russell, E.A., Dewaele, M., Villar, S., Zwolinska, A., Haupt, S., de Lange, J., Yip, D., et al. (2012). MDM4 is a key therapeutic target in cutaneous melanoma. Nat. Med. *18*, 1239–1247.

Gilad, Y., Shiloh, R., Ber, Y., Bialik, S., and Kimchi, A. (2014). Discovering protein-protein interactions within the programmed cell death network using a protein-fragment complementation screen. Cell Rep *8*, 909–921.

Graves, B., Thompson, T., Xia, M., Janson, C., Lukacs, C., Deo, D., Di Lello, P., Fry, D., Garvie, C., Huang, K.S., et al. (2012). Activation of the p53 pathway by small-molecule-induced MDM2 and MDMX dimerization. Proc. Natl. Acad. Sci. USA *109*, 11788–11793.

Green, J.L., Bauer, M., Yum, K.W., Li, Y.C., Cox, M.L., Willert, K., and Wahl, G.M. (2013). Use of a molecular genetic platform technology to produce human Wnt proteins reveals distinct local and distal signaling abilities. PLoS ONE *8*, e58395.

Herce, H.D., Deng, W., Helma, J., Leonhardt, H., and Cardoso, M.C. (2013). Visualization and targeted disruption of protein interactions in living cells. Nat Commun *4*, 2660.

Hodson, C., Cole, A.R., Lewis, L.P., Miles, J.A., Purkiss, A., and Walden, H. (2011). Structural analysis of human FANCL, the E3 ligase in the Fanconi anemia pathway. J. Biol. Chem. *286*, 32628–32637.

Hodson, C., Purkiss, A., Miles, J.A., and Walden, H. (2014). Structure of the human FANCL RING-Ube2T complex reveals determinants of cognate E3-E2 selection. Structure *22*, 337–344.

Ilagan, M.X., Lim, S., Fulbright, M., Piwnica-Worms, D., and Kopan, R. (2011). Real-time imaging of notch activation with a luciferase complementation-based reporter. Sci. Signal. *4*, rs7.

Ivanov, A.A., Khuri, F.R., and Fu, H. (2013). Targeting protein-protein interactions as an anticancer strategy. Trends Pharmacol. Sci. *34*, 393–400.

Joerger, A.C., and Fersht, A.R. (2008). Structural biology of the tumor suppressor p53. Annu. Rev. Biochem. *77*, 557–582.

Lee, J.H., Zhang, Q., Jo, S., Chai, S.C., Oh, M., Im, W., Lu, H., and Lim, H.S. (2011). Novel pyrrolopyrimidine-based α-helix mimetics: cell-permeable inhibitors of protein–protein interactions. J. Am. Chem. Soc. *133*, 676–679.

Levy, E.D., Kowarzyk, J., and Michnick, S.W. (2014). High-resolution mapping of protein concentration reveals principles of proteome architecture and adaptation. Cell Rep *7*, 1333–1340.

Liu, M., Li, C., Pazgier, M., Li, C., Mao, Y., Lv, Y., Gu, B., Wei, G., Yuan, W., Zhan, C., et al. (2010). D-peptide inhibitors of the p53-MDM2 interaction for targeted molecular therapy of malignant neoplasms. Proc. Natl. Acad. Sci. USA *107*, 14321–14326.

Luker, K.E., Smith, M.C., Luker, G.D., Gammon, S.T., Piwnica-Worms, H., and Piwnica-Worms, D. (2004). Kinetics of regulated protein-protein interactions revealed with firefly luciferase complementation imaging in cells and living animals. Proc. Natl. Acad. Sci. USA *101*, 12288–12293.

Macdonald-Obermann, J.L., Piwnica-Worms, D., and Pike, L.J. (2012). Mechanics of EGF receptor/ErbB2 kinase activation revealed by luciferase fragment complementation imaging. Proc. Natl. Acad. Sci. USA *109*, 137–142.

Machida, Y.J., Machida, Y., Chen, Y., Gurtan, A.M., Kupfer, G.M., D'Andrea, A.D., and Dutta, A. (2006). UBE2T is the E2 in the Fanconi anemia pathway and undergoes negative autoregulation. Mol. Cell *23*, 589–596.

Magzoub, M., Oglecka, K., Pramanik, A., Göran Eriksson, L.E., and Gräslund, A. (2005). Membrane perturbation effects of peptides derived from the N-termini of unprocessed prion proteins. Biochim. Biophys. Acta *1716*, 126–136.

Michnick, S.W., Ear, P.H., Manderson, E.N., Remy, I., and Stefan, E. (2007). Universal strategies in research and drug discovery based on protein-fragment complementation assays. Nat. Rev. Drug Discov. *6*, 569–582.

Moldovan, G.L., and D'Andrea, A.D. (2009). How the fanconi anemia pathway guards the genome. Annu. Rev. Genet. *43*, 223–249.

Okamoto, T., Zobel, K., Fedorova, A., Quan, C., Yang, H., Fairbrother, W.J., Huang, D.C., Smith, B.J., Deshayes, K., and Czabotar, P.E. (2013). Stabilizing the pro-apoptotic BimBH3 helix (BimSAHB) does not necessarily enhance affinity or biological activity. ACS Chem. Biol. *8*, 297–302.

Okamoto, T., Segal, D., Zobel, K., Fedorova, A., Yang, H., Fairbrother, W.J., Huang, D.C., Smith, B.J., Deshayes, K., and Czabotar, P.E. (2014). Further insights into the effects of pre-organizing the BimBH3 helix. ACS Chem. Biol. *9*, 838–839.

Patton, J.T., Mayo, L.D., Singhi, A.D., Gudkov, A.V., Stark, G.R., and Jackson, M.W. (2006). Levels of HdmX expression dictate the sensitivity of normal and transformed cells to Nutlin-3. Cancer Res. *66*, 3169–3176.

Paulmurugan, R., and Gambhir, S.S. (2007). Combinatorial library screening for developing an improved split-firefly luciferase fragment-assisted complementation system for studying protein-protein interactions. Anal. Chem. *79*, 2346–2353.

Pazgier, M., Liu, M., Zou, G., Yuan, W., Li, C., Li, C., Li, J., Monbo, J., Zella, D., Tarasov, S.G., and Lu, W. (2009). Structural basis for high-affinity peptide inhibition of p53 interactions with MDM2 and MDMX. Proc. Natl. Acad. Sci. USA *106*, 4665–4670.

Reed, D., Shen, Y., Shelat, A.A., Arnold, L.A., Ferreira, A.M., Zhu, F., Mills, N., Smithson, D.C., Regni, C.A., Bashford, D., et al. (2010). Identification and characterization of the first small molecule inhibitor of MDMX. J. Biol. Chem. *285*, 10786–10796.

Rossi, F.M., Kringstein, A.M., Spicher, A., Guicherit, O.M., and Blau, H.M. (2000). Transcriptional control: rheostat converted to on/off switch. Mol. Cell *6*, 723–728.

Söderberg, O., Gullberg, M., Jarvius, M., Ridderstråle, K., Leuchowius, K.J., Jarvius, J., Wester, K., Hydbring, P., Bahram, F., Larsson, L.G., and Landegren, U. (2006). Direct observation of individual endogenous protein complexes in situ by proximity ligation. Nat. Methods *3*, 995–1000.

Stumpf, M.P., Thorne, T., de Silva, E., Stewart, R., An, H.J., Lappe, M., and Wiuf, C. (2008). Estimating the size of the human interactome. Proc. Natl. Acad. Sci. USA *105*, 6959–6964.

Vassilev, L.T., Vu, B.T., Graves, B., Carvajal, D., Podlaski, F., Filipovic, Z., Kong, N., Kammlott, U., Lukacs, C., Klein, C., et al. (2004). In vivo activation of the p53 pathway by small-molecule antagonists of MDM2. Science *303*, 844–848.

Venkatesan, K., Rual, J.F., Vazquez, A., Stelzl, U., Lemmens, I., Hirozane-Kishikawa, T., Hao, T., Zenkner, M., Xin, X., Goh, K.I., et al. (2009). An empirical framework for binary interactome mapping. Nat. Methods *6*, 83–90.

Verdine, G.L., and Hilinski, G.J. (2012). Stapled peptides for intracellular drug targets. Methods Enzymol. *503*, 3–33.

Wade, M., Rodewald, L.W., Espinosa, J.M., and Wahl, G.M. (2008). BH3 activation blocks Hdmx suppression of apoptosis and cooperates with Nutlin to induce cell death. Cell Cycle *7*, 1973–1982.

Wade, M., Li, Y.C., and Wahl, G.M. (2013). MDM2, MDMX and p53 in oncogenesis and cancer therapy. Nat. Rev. Cancer *13*, 83–96.

Wadia, J.S., Stan, R.V., and Dowdy, S.F. (2004). Transducible TAT-HA fusogenic peptide enhances escape of TAT-fusion proteins after lipid raft macropinocytosis. Nat. Med. *10*, 310–315.

Wells, J.A., and McClendon, C.L. (2007). Reaching for high-hanging fruit in drug discovery at protein-protein interfaces. Nature *450*, 1001–1009.

Wong, E.T., Kolman, J.L., Li, Y.C., Mesner, L.D., Hillen, W., Berens, C., and Wahl, G.M. (2005). Reproducible doxycycline-inducible transgene expression at specific loci generated by Cre-recombinase mediated cassette exchange. Nucleic Acids Res. *33*, e147.

Yang, K.S., Ilagan, M.X., Piwnica-Worms, D., and Pike, L.J. (2009). Luciferase fragment complementation imaging of conformational changes in the epidermal growth factor receptor. J. Biol. Chem. *284*, 7474–7482.

Ye, Y., and Rape, M. (2009). Building ubiquitin chains: E2 enzymes at work. Nat. Rev. Mol. Cell Biol. *10*, 755–764.